Distributed Space-Time Block Coding for Barrage Relay Networks

Ki-Hun Lee*, Howon Lee†, Jungwook Choi‡, Soobum Park‡, and Bang Chul Jung*
*Department of Electronics Engineering, Chungnam National University, Daejeon, South Korea
†School of Electronic and Electrical Engineering and IITC, Hankyong National University, Anseong, South Korea
‡LIG Nex1 Co., Ltd., Yongin-si, Gyeonggi-do, South Korea
Email: kihun.h.lee@cnu.ac.kr, hwlee@hknu.ac.kr, jungwook.choi2@lignex.com, sbpark93@lignex1.com, bcjung@cnu.ac.kr

MILCOM 2023 - 2023 IEEE Military Communications Conference (MILCOM) | 979-8-3503-2181-4/23/$31.00 ©2023 IEEE | DOI: 10.1109/MILCOM58377.2023.10356386

***Abstract*—We propose a fully distributed space-time block coding (FD-STBC) technique for *barrage relay networks* (BRNs) which is specifically designed for military tactical mobile ad hoc networks (MANETs). The BRNs are based on a rapid and robust flooding protocol with two network capabilities: time-division multiple access (TDMA) and autonomous cooperative communication, whereby relays' simultaneous transmission of common packets results in cooperative diversity. Unfortunately, however, the existing phase rotation (PR)-based cooperation scheme cannot exploit the spatial diversity gain. Therefore, we apply the FD-STBC instead of the PR to relays, especially exploiting a complex hypersphere-based randomization matrix. It is noteworthy that the proposed FD-STBC-based BRN remarkably outperforms the conventional BRN even in a network with only two relays. Furthermore, we mathematically analyze the end-to-end performance of the proposed FD-STBC-based BRN in terms of outage probability.**

***Index Terms*—Barrage relay networks, fully distributed space-time block coding, military tactical mobile ad hoc networks, outage probability, randomized space-time coding.**

I. Introduction

Originating from the network-centric warfare paradigm, modern military tactical communication systems usually operate in areas with no fixed infrastructure and are envisioned as completely decentralized mobile ad hoc networks (MANETs) consisting of heterogeneous units such as dismounted soldiers, ground vehicles, and aerial platforms [1]–[5]. In addition, with the proliferation of the civilian internet-of-things (IoT), military IoT applications called internet-of-battlefield things (IoBT) are also increasing proportionally to realize intelligent networked battlefield systems [6], [7]. The IoBT connects massive smart tactical devices to a battlefield network, generates large-scale information, such as real-time images, videos, and sensor data, and coordinates complex combat operations [8]. In other words, future tactical MANETs must be able to withstand network dynamics and massive connectivity with high reliability, scalability, and low latency.

The barrage relay network (BRN) is a broadcast-oriented cooperative MANET system originally designed for tactical MANETs to fulfill the aforementioned requirements [5], [9], [10]. BRNs are based on a rapid and robust flooding protocol with two underlying network capabilities: time-division multiple access (TDMA) and autonomous cooperative communication without point-to-point link abstraction. All nodes in the network adopt a common TDMA frame structure with coarse slot-level synchronization, and concurrent transmission of identical packets results in cooperative diversity, not collisions. The BRNs can eliminate the need for channel access and routing protocols in the networks and allow massive connectivity with low overhead. Unicast transmission can also be supported via the same barrage flooding mechanism [10]–[12]. In particular, multiple unicast flows within a BRN can be spatially separated and simultaneously transmitted by forming controlled barrage regions (CBRs), where a CBR is established by identifying a ring of buffer nodes that isolate internal cooperating nodes, including a source and its destination. The interior relays aid in relaying data packets between the source and the destination, and buffers suppress their relay function, enabling concurrent unicast transmissions in different subregions within the entire network. More recently, the suitability of BRNs for higher dense networks, the trade-off between reliability and node utilization, geometric analysis of CBR, transmit power scaling, and time synchronization have been investigated in the literature [13]–[15].

On the other hand, randomized space-time codes (RSTCs) have been proposed in [16] for entirely decentralized cooperative communications. The basic idea of the RSTC is to induce spatial diversity and coding gains by leveraging distributed cooperating nodes in an ad hoc network or a distributed antenna system as multiple transmit antennas without extra centralized procedure. To be specific, each cooperating node that correctly decodes the source message maps that common packet onto the same predefined space-time block code (STBC) matrix and then transmits it in linear combination with its randomization vector independently and randomly selected from an identical distribution.[1] It is worth noting that applying conventional distributed space-time codes (DSTCs) [17], [18] to BRNs has been considered infeasible as it requires central control or inter-node coordination resulting in significant signaling overhead and latency [5], [10]. However, the RSTCs can

This work was partly supported by the Korea Research Institute for Defense Technology Planning and Advancement-Grant funded by the Defense Acquisition Program Administration (DAPA) (KRIT-CT-21-030) and the National Research Foundation of Korea (NRF) grant funded by the Korea government (MSIT) (No. NRF-2021R1A4A1032580).

[1] In this vein, in this paper, we refer to this scheme as *fully distributed space-time block coding* (FD-STBC) to highlight its characteristics more intuitively.

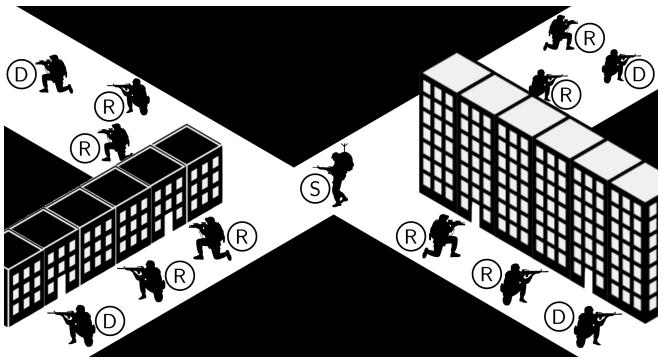

Fig. 1. A BRN of tactical MANET consisting of a source (S), multiple receiving nodes (R, D) on four junctions.

operate independently for each node in a fully distributed manner without such coordination.

This motivates us to investigate an FD-STBC-based BRN, especially one with a randomization matrix selected on the surface of a complex hypersphere. To the best of our knowledge, this study is the first work to apply the FD-STBC in BRNs. Furthermore, although an RSTC with a randomization matrix consisting of independent and identically distributed columns that are *uniformly distributed on a complex unit hypersphere* achieves the best performance and is practical in the perspective of average transmission power normalization, the performance analysis has not been investigated [19], [20]. We mathematically analyze the end-to-end outage probability performance of the proposed FD-STBC-based BRN. In other words, we further present a novel analytical result for the FD-STBC.

II. System Model

To validate the effectiveness of FD-STBC in BRNs and for the sake of brevity, in this paper, we consider a simple BRN to which the FD-STBC can be applied, as illustrated in Fig. 1. There is one source node in the center that broadcasts a message, and each of the four zones has three communication nodes that receive the common message. All nodes here are equipped with a single antenna. Furthermore, it is assumed that received signal strengths (RSSs) between streets are negligible due to blockages. Each branch can then be regarded equivalently as a four-node CBR consisting of a source (S), a destination (D), and two relays (R_k, $k \in \{1,2\}$). A packet is propagated outward from the source with decode-and-forward protocols [21], [22]. Each relay relays the packet only once to prevent its transmission from propagating back toward the source. Accordingly, the maximum number of time slots per TDMA frame is three in this BRN topology [10], [11].

From now on, without loss of generality, we consider one branch within the BRN, i.e., the aforementioned four-node CBR with $\{\mathsf{S}, \mathsf{R}_1, \mathsf{R}_2, \mathsf{D}\}$. We define three sets for each time slot $t \in \{1,2,3\}$ to indicate the node state as in [11], [12]:

- $\mathcal{R}^{(t)}$ is the set of *ready* nodes that have not yet successfully decoded the packet in slot t; and obviously, $\mathcal{R}^{(1)} = \{\mathsf{R}_1, \mathsf{R}_2, \mathsf{D}\}$.
- $\mathcal{A}^{(t)}$ is the set of *active* nodes that have received and decoded the packet in slot $t-1$ and will broadcast it in slot t; and $\mathcal{A}^{(1)} = \{\mathsf{S}\}$.
- $\mathcal{S}^{(t)}$ is the set of *sleep* nodes that decoded and transmitted the packet before slot t and will no longer transmit or receive that packet; $\mathcal{S}^{(1)} = \varnothing$.

Let $\mathbf{x}$ $(= [x_1, x_2, \dots x_N]^{\mathrm{T}})$ be a packet of source symbols to broadcast, where N represents the packet length. Herein, we focus on the first two consecutive symbols in the packet for the convenience of exposition without loss of generality; hence, $\mathbf{x} = [x_1, x_2]^{\mathrm{T}}$. This is also because there are two relays, so the maximum achievable diversity order of the FD-STBC is two [16]. Furthermore, we assume block fading channels for at least two symbol times, i.e., the wireless channels within the network remain constant for a time slot but vary independently from slot to slot. This assumption is sufficiently practical in that the network topology dynamics over time are much slower than fading in general [12]. Finally, it is also assumed that all nodes are perfectly synchronized [16]. The BRN flooding primitive for each branch works as follows.

A. First slot

In the first slot of a TDMA frame, the source broadcasts a packet $\mathbf{x}$. The received signals at the relays and destination, denoted by $\mathbf{y}_j^{(1)}$ $(= [y_{j,1}^{(1)}, y_{j,2}^{(1)}]^{\mathrm{T}})$, are then given as follows:

$$\mathbf{y}_j^{(1)} = \sqrt{P_{\mathsf{S}}}\sqrt{d_{j,\mathsf{S}}^{-\alpha}}\widetilde{h}_{j,\mathsf{S}}^{(1)}\mathbf{x} + \mathbf{w}_j^{(1)},\ \forall j \in \mathcal{R}^{(1)}, \tag{1}$$

where P_i $(= P)$ is the average transmission power of node $i \in \mathcal{A}^{(t)}$, and we assume the same average power of P for all nodes; $d_{j,i}^{-\alpha}$ represents the large-scale fading component with the distance between nodes j and i, $d_{j,i}$, and the path loss exponent, α; $\widetilde{h}_{j,i}^{(t)}$ denotes the small-scale fading component between nodes j and i at slot t which is assumed to follow an independent and identically distributed (i.i.d.) zero-mean ant unit-variance complex circularly symmetric Gaussian distribution, i.e., $\widetilde{h}_{j,i}^{(t)} \sim \mathcal{CN}(0,1)$. Let $h_{j,i}^{(t)} = \sqrt{d_{j,i}^{-\alpha}}\widetilde{h}_{j,i}^{(t)}$ be the wireless channel between nodes j and i at slot t, i.e., $h_{j,i}^{(t)} \sim \mathcal{CN}(0, \sigma_{j,i})$ and $|h_{j,i}^{(t)}|^2 \sim \exp(1/\sigma_{j,i})$, where $\sigma_{j,i} = d_{j,i}^{-\alpha}$. Finally, $\mathbf{w}_j^{(t)}$ is the additive white Gaussian noise (AWGN) at $\mathbf{y}_j^{(t)}$, i.e., $\mathbf{w}_j^{(t)} \sim \mathcal{CN}(\mathbf{0}, N_0\mathbf{I}_2)$, where N_0 is the noise power and $\mathbf{I}_n$ denotes $n \times n$ identity matrix.

From (1), the received signal-to-noise ratio (SNR) of node j at the first slot is derived as $\rho_j^{(1)} = P|h_{j,\mathsf{S}}^{(1)}|^2/N_0 = \rho_0|h_{j,\mathsf{S}}^{(1)}|^2$, where $\rho_j^{(t)}$ denotes the instantaneous received SNR of node j at slot t and $\rho_0 := P/N_0$ is the average transmit SNR. The node state sets are then updated as

- $\mathcal{R}^{(2)} = \{j \mid \rho_j^{(1)} < \rho_{\mathsf{th}}, j \in \mathcal{R}^{(1)}\}$,
- $\mathcal{A}^{(2)} = \{j \mid \rho_j^{(1)} \geq \rho_{\mathsf{th}}, j \in \mathcal{R}^{(1)}\}$,
- $\mathcal{S}^{(2)} = \mathcal{A}^{(1)} = \{\mathsf{S}\}$,

where ρ_{th} represents the threshold SNR required for reliable reception, i.e., an outage occurs when the SNR falls below it. Note that the destination can also receive the source message directly if $\rho_{\mathsf{D}}^{(1)} \geq \rho_{\mathsf{th}}$ [11].

B. Second slot

During the second slot, the nodes that have reliably decoded the initial transmission rebroadcast the packet. Existing BRNs exploit phase rotations (PRs) in [23] as an autonomous cooperative communication scheme. The received signals at each node $j \in \mathcal{R}^{(2)}$, denoted by $\widetilde{\mathbf{y}}_j^{(2)}$ $(= [\widetilde{y}_{j,1}^{(2)}, \widetilde{y}_{j,2}^{(2)}]^{\mathrm{T}})$, can then be written as follows [13], [24]:

$$\widetilde{\mathbf{y}}_j^{(2)} = \sum_{i \in \mathcal{A}^{(2)}} \sqrt{P} h_{j,i}^{(2)} e^{j\theta_i} \mathbf{x} + \mathbf{w}_j^{(2)}, \ \forall j \in \mathcal{R}^{(2)}, \tag{2}$$

where θ_i follows an i.i.d. uniform distribution with $\theta_i \sim \mathcal{U}[0, 2\pi)$. That is, node $i \in \mathcal{A}^{(2)}$ relays the packet with a random phase θ_i. From the properties of the circularly symmetric Gaussian of the wireless channel, $h_{j,i}^{(t)} e^{j\theta_i} \sim \mathcal{CN}(0, \sigma_{j,i})$.

On the other hand, when FD-STBC is applied, the received signals at node $j \in \mathcal{R}^{(2)}$, denoted by $\mathbf{y}_j^{(2)}$ $(= [y_{j,1}^{(2)}, y_{j,2}^{(2)}]^{\mathrm{T}})$, are given as follows [16], [20]:

$$\begin{aligned} \mathbf{y}_j^{(2)} &= \sum_{i \in \mathcal{A}^{(2)}} \sqrt{P} h_{j,i}^{(2)} \mathcal{B}(\mathbf{x}) \mathbf{r}_i + \mathbf{w}_j^{(2)} \\ &= \sqrt{P} \mathcal{B}(\mathbf{x}) \mathbf{R}^{(2)} \mathbf{h}_j^{(2)} + \mathbf{w}_j^{(2)}, \ \forall j \in \mathcal{R}^{(2)}, \end{aligned} \tag{3}$$

where $\mathcal{B}(\mathbf{x})$ is an $S \times L$ common space-time block coding (STBC) encoder for the packet $\mathbf{x}$, and in this paper, we exploit the well-known Alamouti code with $S = L = 2$ given by

$$\mathcal{B}(\mathbf{x}) = \begin{bmatrix} x_1 & x_2 \\ -x_2^* & x_1^* \end{bmatrix}, \tag{4}$$

where rows and columns correspond to the symbol times in a slot and the transmit antenna indices in the underlying space-time code, respectively; $\mathbf{h}_j^{(t)} = [h_{j,i}^{(t)}] \in \mathbb{C}^{|\mathcal{A}^{(t)}| \times 1}$ denotes the channel vector consisting of the receive channel coefficients of node $j \in \mathcal{R}^{(t)}$. Furthermore, $\mathbf{R}^{(t)} = [\mathbf{r}_i] \in \mathbb{C}^{L \times |\mathcal{A}^{(t)}|}$ denotes the *randomization matrix*, where $\mathbf{r}_i = [r_{i,1}, r_{i,2}]^{\mathrm{T}} \in \mathbb{C}^{2 \times 1}$ is a randomization vector of node $i \in \mathcal{A}^{(t)}$, which is independently chosen from the surface of a complex unit hypersphere; e.g.,

$$r_{i,1} = \frac{\widetilde{r}_{i,1}}{\sqrt{|\widetilde{r}_{i,1}|^2 + |\widetilde{r}_{i,2}|^2}}, \ r_{i,2} = \frac{\widetilde{r}_{i,2}}{\sqrt{|\widetilde{r}_{i,1}|^2 + |\widetilde{r}_{i,2}|^2}}, \tag{5}$$

where $\widetilde{r}_{i,l} \sim \mathcal{CN}(0, 1)$.

From the two received signals in (3), node j performs STBC decoding as follows:

$$\begin{aligned} \overline{\mathbf{y}}_j^{(2)} &= \frac{1}{\|\widehat{\mathbf{h}}_j^{(2)}\|} \begin{bmatrix} \left(\widehat{h}_{j,1}^{(2)}\right)^* & \widehat{h}_{j,2}^{(2)} \\ \left(\widehat{h}_{j,2}^{(2)}\right)^* & -\widehat{h}_{j,1}^{(2)} \end{bmatrix} \begin{bmatrix} y_{j,1}^{(2)} \\ \left(y_{j,2}^{(2)}\right)^* \end{bmatrix} \\ &= \sqrt{P} \|\widehat{\mathbf{h}}_j^{(2)}\| \mathbf{x} + \widetilde{\mathbf{w}}_j^{(2)} = \sqrt{P} \|\mathbf{R}^{(2)} \mathbf{h}_j^{(2)}\| \mathbf{x} + \widetilde{\mathbf{w}}_j^{(2)}, \end{aligned} \tag{6}$$

where $\widehat{\mathbf{h}}_j^{(t)} = [\widehat{h}_{j,1}^{(t)}, \widehat{h}_{j,2}^{(t)}]^{\mathrm{T}} = \mathbf{R}^{(t)} \mathbf{h}_j^{(t)}$ represents the effective channel of node j at slot t when the FD-STBC is exploited, and the noise $\widetilde{\mathbf{w}}_j^{(t)}$ still follows $\mathcal{CN}(\mathbf{0}, N_0 \mathbf{I}_2)$. Since the two symbols in (6), x_1 and x_2, can be independently decoded (symbol-wise decoding), the received SNR of node j at the second slot is given by $\rho_j^{(2)} = \rho_0 \|\mathbf{R}^{(2)} \mathbf{h}_j^{(2)}\|^2$.

Let us compare the received signals, (2) and (6), on the destination side. Note that $\mathsf{S} \notin \mathcal{A}^{(2)}$. If only one of the two relays reliably decoded the source message in the first slot, the received SNRs at the destination in the second slot are respectively given by

$$\rho_{\mathsf{D}}^{(2)} = \begin{cases} \rho_0 |h_{\mathsf{D},i}^{(2)} e^{j\theta_i}|^2 = \rho_0 |h_{\mathsf{D},i}^{(2)}|^2, & \text{for PR,} \\ \rho_0 \sum_{l=1}^{2} |r_{i,l} h_{\mathsf{D},i}^{(2)}|^2 = \rho_0 |h_{\mathsf{D},i}^{(2)}|^2, & \text{for FD-STBC.} \end{cases} \tag{7}$$

Therefore, the wireless channel gain is the same. On the other hand, if both relays reliably decoded the source message in the first slot, they are given by

$$\rho_{\mathsf{D}}^{(2)} = \begin{cases} \rho_0 |h_{\mathsf{D},\mathsf{R}_1}^{(2)} + h_{\mathsf{D},\mathsf{R}_2}^{(2)}|^2, & \text{for PR,} \\ \rho_0 \sum_{l=1}^{2} \left| \sum_{i \in \{\mathsf{R}_1, \mathsf{R}_2\}} r_{i,l} h_{\mathsf{D},i}^{(2)} \right|^2, & \text{for FD-STBC.} \end{cases} \tag{8}$$

We will mathematically analyze the difference in performance with these channel gains in Section III.

It is noteworthy that since each node independently selects its random vector, there is no central control or inter-node coordination. Moreover, the receiver does not need to know the number of cooperative nodes and their respective random vectors and channel state information (CSI). The receiver only requires the equivalent channel coefficients $\widehat{\mathbf{h}}_j^{(t)}$ that can be estimated via pilot signals [19], [20], which has the same burden as the conventional PR-based BRN. In other words, the proposed FD-STBC-based BRN can be implemented in a completely decentralized fashion. The node state sets are finally updated as

- $\mathcal{R}^{(3)} = \{j \mid \rho_j^{(2)} < \rho_{\mathsf{th}}, j \in \mathcal{R}^{(2)}\}$,
- $\mathcal{A}^{(3)} = \{j \mid \rho_j^{(2)} \geq \rho_{\mathsf{th}}, j \in \mathcal{R}^{(2)}\}$,
- $\mathcal{S}^{(3)} = \mathcal{S}^{(2)} \cup \mathcal{A}^{(2)}$.

C. Third slot

In the third (final) slot, the node that have successfully decoded the packet at the end of the previous slot rebroadcasts it. From the destination side, we can expect that only one of the two relays remains in this slot or no one is left. Based on the same procedure as in the second slot, the received signals at the destination are given from (2) and (6) as

$$\widetilde{\mathbf{y}}_{\mathsf{D}}^{(3)} = \sqrt{P} h_{\mathsf{D},i}^{(3)} e^{j\theta_i} \mathbf{x} + \mathbf{w}_{\mathsf{D}}^{(3)}, \ i \in \mathcal{A}^{(3)}, \text{ for PR,} \tag{9}$$

and

$$\overline{\mathbf{y}}_{\mathsf{D}}^{(3)} = \sqrt{P} \|\mathbf{r}_i h_{\mathsf{D},i}^{(3)}\| \mathbf{x} + \widetilde{\mathbf{w}}_{\mathsf{D}}^{(3)}, \ i \in \mathcal{A}^{(3)}, \text{ for FD-STBC,} \tag{10}$$

respectively. Therefore, the received SNR of the destination is derived as $\rho_{\mathsf{D}}^{(3)} = \rho_0 |h_{\mathsf{D},i}^{(3)}|^2$ for both cases. If $\mathsf{D} \in \mathcal{R}^{(3)}$ and $\rho_{\mathsf{D}}^{(3)} < \rho_{\mathsf{th}}$, this means that an end-to-end outage has occurred.

III. Performance Analysis

In this section, we mathematically analyze the end-to-end outage probability of the proposed FD-STBC-based BRN for a given topology, especially the considered four-node CBR. The outage probability is the probability that the instantaneous received SNR falls below a certain threshold ρ_{th}.

First of all, if only one node i sent the packet at slot t, the outage probability of node j $(\neq i)$ is defined as

$$\epsilon_{j,i}^{(t)} = \Pr\left(\rho_j^{(t)} < \rho_{\mathsf{th}} \mid \sigma_{j,i}\right) = \Pr\left(|h_{j,i}^{(t)}|^2 < \frac{\rho_{\mathsf{th}}}{\rho_0}\middle|\sigma_{j,i}\right). \quad (11)$$

Since the probability density function of $|h_{j,i}^{(t)}|^2$ is given by

$$f_{|h_{j,i}^{(t)}|^2}(y) = \frac{1}{\sigma_{j,i}} \exp(-\frac{y}{\sigma_{j,i}}),$$

the outage probability for a single-node transmission is derived as follows:

$$\epsilon_{j,i}^{(t)} = \int_0^{\frac{\rho_{\mathsf{th}}}{\rho_0}} \frac{1}{\sigma_{j,i}} \exp\left(-\frac{y}{\sigma_{j,i}}\right) dy = 1 - \exp\left(-\frac{\rho_{\mathsf{th}}}{\rho_0 \sigma_{j,i}}\right), \quad (12)$$

regardless of using PR or FD-STBC.

Meanwhile, in the second slot, we have observed the case that the destination receives the simultaneous transmission of both relays, in which case the outage probability can be defined as

$$\epsilon_{\mathsf{D},\{\mathsf{R}_1,\mathsf{R}_2\}}^{(2)} = \Pr\left(\rho_{\mathsf{D}}^{(2)} < \rho_{\mathsf{th}} \middle| \sigma_{\mathsf{D},\mathsf{R}_1}, \sigma_{\mathsf{D},\mathsf{R}_2}\right). \quad (13)$$

For conventional BRNs using PRs, the outage probability in this case is derived from (8) for PR as follows[2]:

$$\epsilon_{\mathsf{D},\{\mathsf{R}_1,\mathsf{R}_2\}}^{(2)} = 1 - \exp\left(-\frac{\rho_{\mathsf{th}}}{\rho_0(\sigma_{\mathsf{D},\mathsf{R}_1} + \sigma_{\mathsf{D},\mathsf{R}_2})}\right). \quad (14)$$

On the other hand, with FD-STBC, the received SNR is given by $\rho_0 \|\mathbf{R}^{(2)}\mathbf{h}_{\mathsf{D}}^{(2)}\|^2$ and (8) for FD-STBC. We exploit an upper bound for the tractable analysis. First of all, we can equivalently consider $\|\mathbf{R}\mathbf{\Sigma}^{1/2}\widetilde{\mathbf{h}}\|^2$ instead of $\|\mathbf{R}^{(2)}\mathbf{h}_{\mathsf{D}}^{(2)}\|^2$, where $\mathbf{R} := \mathbf{R}^{(2)}$, $\mathbf{\Sigma} = \mathrm{diag}(\sigma_{\mathsf{D},\mathsf{R}_1}, \sigma_{\mathsf{D},\mathsf{R}_2})$, and $\widetilde{\mathbf{h}} := \widetilde{\mathbf{h}}_{\mathsf{D}}^{(2)} = [\widetilde{h}_{\mathsf{D},\mathsf{R}_1}^{(2)}, \widetilde{h}_{\mathsf{D},\mathsf{R}_2}^{(2)}]^{\mathrm{T}} \sim \mathcal{CN}(\mathbf{0}, \mathbf{I}_2)$. Let $\mathbf{U}^{\mathrm{H}}\mathbf{\Lambda}\mathbf{U}$ be the eigenvalue decomposition of $\mathbf{\Sigma}^{1/2}\mathbf{R}^{\mathrm{H}}\mathbf{R}\mathbf{\Sigma}^{1/2}$, where $\mathbf{U}$ is a unitary matrix and $\mathbf{\Lambda} = \mathrm{diag}(\lambda_1^2, \lambda_2^2)$ is a diagonal matrix composed of the ordered eigenvalues $(\lambda_1 \geq \lambda_2 > 0)$. From [16, (6)], the outage probability for this case can be derived as

$$\begin{aligned}\epsilon_{\mathsf{D},\{\mathsf{R}_1,\mathsf{R}_2\}}^{(2)} &= \Pr\left(\rho_{\mathsf{D}}^{(2)} < \rho_{\mathsf{th}} \mid \sigma_{\mathsf{D},\mathsf{R}_1}, \sigma_{\mathsf{D},\mathsf{R}_2}\right) \\ &= \Pr\left(\rho_0 \|\mathbf{R}^{(2)}\mathbf{h}_{\mathsf{D}}^{(2)}\|^2 < \rho_{\mathsf{th}} \mid \sigma_{\mathsf{D},\mathsf{R}_1}, \sigma_{\mathsf{D},\mathsf{R}_2}\right) \\ &= \Pr\left(\sum_{k=1}^{2} \lambda_k^2 |\widetilde{h}_{\mathsf{D},\mathsf{R}_k}^{(2)}|^2 < \frac{\rho_{\mathsf{th}}}{\rho_0}\middle| \sigma_{\mathsf{D},\mathsf{R}_1}, \sigma_{\mathsf{D},\mathsf{R}_2}\right).\end{aligned} \quad (15)$$

Furthermore, this can be upper bounded as (16) at the top of the next page with the probability density functions of λ_1^2 and λ_2^2 given by

$$f_{\lambda_1^2}(x_1) = \frac{8x_1 - 4(\sigma_{\mathsf{D},\mathsf{R}_1} + \sigma_{\mathsf{D},\mathsf{R}_2})}{(\sigma_{\mathsf{D},\mathsf{R}_1} + \sigma_{\mathsf{D},\mathsf{R}_2})^2 - (\sigma_{\mathsf{D},\mathsf{R}_1} - \sigma_{\mathsf{D},\mathsf{R}_2})^2}, \quad \sigma_{\mathsf{D},\mathsf{R}_2} \leq x_1 \leq \sigma_{\mathsf{D},\mathsf{R}_1} + \sigma_{\mathsf{D},\mathsf{R}_2},$$

$$f_{\lambda_2^2}(x_2) = \frac{-8x_2 + 4(\sigma_{\mathsf{D},\mathsf{R}_1} + \sigma_{\mathsf{D},\mathsf{R}_2})}{(\sigma_{\mathsf{D},\mathsf{R}_1} + \sigma_{\mathsf{D},\mathsf{R}_2})^2 - (\sigma_{\mathsf{D},\mathsf{R}_1} - \sigma_{\mathsf{D},\mathsf{R}_2})^2}, \quad 0 \leq x_2 \leq \sigma_{\mathsf{D},\mathsf{R}_1}.$$

[2]The authors in the literature [11], [12] stated that the channel gain is obtained as $|h_{\mathsf{D},\mathsf{R}_1}^{(2)}|^2 + |h_{\mathsf{D},\mathsf{R}_2}^{(2)}|^2$. However, as described in the literature [13], [24], and (8), the channel gain is derived as $|h_{\mathsf{D},\mathsf{R}_1}^{(2)} + h_{\mathsf{D},\mathsf{R}_2}^{(2)}|^2$, which follows an exponential distribution with a rate parameter of $1/(\sigma_{\mathsf{D},\mathsf{R}_1} + \sigma_{\mathsf{D},\mathsf{R}_2})$.

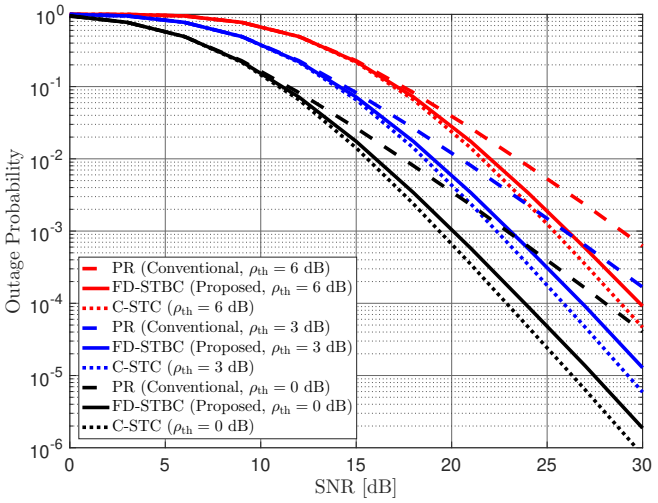

(a) Monte-Carlo simulation

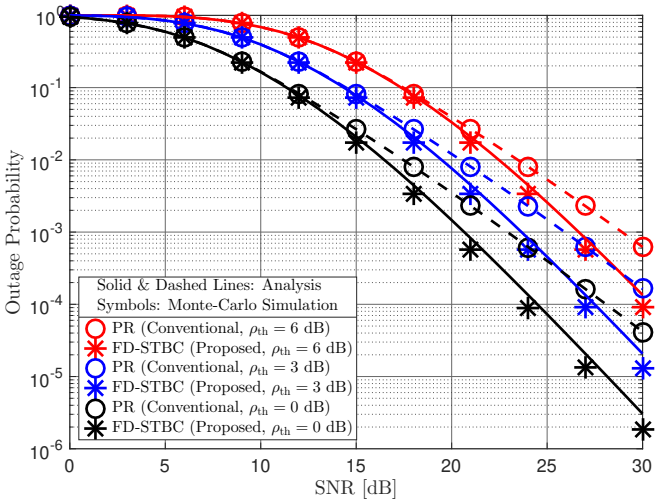

(b) Mathematical analysis

Fig. 2. End-to-end outage probability performance of the conventional PR-based BRN, the proposed FD-STBC-based BRN, and the centralized STC-based BRN in a line-shaped four-node CBR.

Finally, the source message is successfully delivered whenever the destination reliably receives the packet. Using the total probability theorem, the end-to-end *outage probability*, denoted by $\epsilon_{\mathsf{e2e}}\{\mathcal{O}\}$, is defined as follows:

$$\epsilon_{\mathsf{e2e}}\{\mathcal{O}\} = 1 - \epsilon_{\mathsf{e2e}}\{\mathcal{S}\}, \quad (17)$$

where $\epsilon_{\mathsf{e2e}}\{\mathcal{S}\}$ denotes the end-to-end *success probability* which can be defined as

$$\begin{aligned}\epsilon_{\mathsf{e2e}}\{\mathcal{S}\} &= (1 - \epsilon_{\mathsf{D},\mathsf{S}}^{(1)}) \\ &+ \epsilon_{\mathsf{D},\mathsf{S}}^{(1)}(1 - \epsilon_{\mathsf{R}_1,\mathsf{S}}^{(1)})\epsilon_{\mathsf{R}_2,\mathsf{S}}^{(1)}\left[(1 - \epsilon_{\mathsf{D},\mathsf{R}_1}^{(2)}) + \epsilon_{\mathsf{D},\mathsf{R}_1}^{(2)}(1 - \epsilon_{\mathsf{R}_2,\mathsf{R}_1}^{(2)})(1 - \epsilon_{\mathsf{D},\mathsf{R}_2}^{(3)})\right] \\ &+ \epsilon_{\mathsf{D},\mathsf{S}}^{(1)}\epsilon_{\mathsf{R}_1,\mathsf{S}}^{(1)}(1 - \epsilon_{\mathsf{R}_2,\mathsf{S}}^{(1)})\left[(1 - \epsilon_{\mathsf{D},\mathsf{R}_2}^{(2)}) + \epsilon_{\mathsf{D},\mathsf{R}_2}^{(2)}(1 - \epsilon_{\mathsf{R}_1,\mathsf{R}_2}^{(2)})(1 - \epsilon_{\mathsf{D},\mathsf{R}_1}^{(3)})\right] \\ &+ \epsilon_{\mathsf{D},\mathsf{S}}^{(1)}(1 - \epsilon_{\mathsf{R}_1,\mathsf{S}}^{(1)})(1 - \epsilon_{\mathsf{R}_2,\mathsf{S}}^{(1)})(1 - \epsilon_{\mathsf{D},\{\mathsf{R}_1,\mathsf{R}_2\}}^{(2)}).\end{aligned}$$

By substituting (12) and (15) with (16) to (17), an upper bound expression of the end-to-end outage probability for the

$$\Pr\left(\sum_{k=1}^{2}\lambda_k^2|\widetilde{h}_{\mathsf{D},\mathsf{R}_k}^{(2)}|^2<\frac{\rho_{\mathsf{th}}}{\rho_0}\middle|\sigma_{\mathsf{D},\mathsf{R}_k}\right)\le\Pr\left(\lambda_1^2|\widetilde{h}_{\mathsf{D},\mathsf{R}_1}^{(2)}|^2<\frac{\rho_{\mathsf{th}}}{\rho_0},\lambda_2^2|\widetilde{h}_{\mathsf{D},\mathsf{R}_2}^{(2)}|^2<\frac{\rho_{\mathsf{th}}}{\rho_0}\middle|\sigma_{\mathsf{D},\mathsf{R}_1},\sigma_{\mathsf{D},\mathsf{R}_2}\right) \tag{16}$$

$$=\Pr\left(\lambda_1^2|\widetilde{h}_{\mathsf{D},\mathsf{R}_1}^{(2)}|^2<\frac{\rho_{\mathsf{th}}}{\rho_0}\middle|\sigma_{\mathsf{D},\mathsf{R}_1}\right)\Pr\left(\lambda_2^2|\widetilde{h}_{\mathsf{D},\mathsf{R}_2}^{(2)}|^2<\frac{\rho_{\mathsf{th}}}{\rho_0}\middle|\sigma_{\mathsf{D},\mathsf{R}_2}\right)$$

$$=\int_{\sigma_{\mathsf{D},\mathsf{R}_2}}^{\sigma_{\mathsf{D},\mathsf{R}_1}+\sigma_{\mathsf{D},\mathsf{R}_2}}\int_0^{\frac{\rho_{\mathsf{th}}}{\rho_0 x_1}}\exp(-u_1)\frac{8x_1-4(\sigma_{\mathsf{D},\mathsf{R}_1}+\sigma_{\mathsf{D},\mathsf{R}_2})}{(\sigma_{\mathsf{D},\mathsf{R}_1}+\sigma_{\mathsf{D},\mathsf{R}_2})^2-(\sigma_{\mathsf{D},\mathsf{R}_1}-\sigma_{\mathsf{D},\mathsf{R}_2})^2}du_1dx_1$$

$$\times\int_0^{\sigma_{\mathsf{D},\mathsf{R}_1}}\int_0^{\frac{\rho_{\mathsf{th}}}{\rho_0 x_2}}\exp(-u_2)\frac{-8x_2+4(\sigma_{\mathsf{D},\mathsf{R}_1}+\sigma_{\mathsf{D},\mathsf{R}_2})}{(\sigma_{\mathsf{D},\mathsf{R}_1}+\sigma_{\mathsf{D},\mathsf{R}_2})^2-(\sigma_{\mathsf{D},\mathsf{R}_1}-\sigma_{\mathsf{D},\mathsf{R}_2})^2}du_2dx_2$$

$$=\left[\frac{\frac{\rho_{\mathsf{th}}}{\rho_0}\left(\sigma_{\mathsf{D},\mathsf{R}_1}+\sigma_{\mathsf{D},\mathsf{R}_2}+\frac{\rho_{\mathsf{th}}}{\rho_0}\right)\mathrm{Ei}\left(\frac{\rho_{\mathsf{th}}}{\rho_0\sigma_{\mathsf{D},\mathsf{R}_2}}\right)-\sigma_{\mathsf{D},\mathsf{R}_2}\left(\sigma_{\mathsf{D},\mathsf{R}_1}+\frac{\rho_{\mathsf{th}}}{\rho_0}\right)\exp\left(-\frac{\rho_{\mathsf{th}}}{\rho_0\sigma_{\mathsf{D},\mathsf{R}_2}}\right)+\sigma_{\mathsf{D},\mathsf{R}_1}\sigma_{\mathsf{D},\mathsf{R}_2}}{\sigma_{\mathsf{D},\mathsf{R}_1}\sigma_{\mathsf{D},\mathsf{R}_2}}\right.$$

$$\left.-\frac{\frac{\rho_{\mathsf{th}}}{\rho_0}\left(\sigma_{\mathsf{D},\mathsf{R}_1}+\sigma_{\mathsf{D},\mathsf{R}_2}+\frac{\rho_{\mathsf{th}}}{\rho_0}\right)\mathrm{Ei}\left(\frac{\rho_{\mathsf{th}}}{\rho_0(\sigma_{\mathsf{D},\mathsf{R}_1}+\sigma_{\mathsf{D},\mathsf{R}_2})}\right)-\frac{\rho_{\mathsf{th}}}{\rho_0}(\sigma_{\mathsf{D},\mathsf{R}_1}+\sigma_{\mathsf{D},\mathsf{R}_2})\exp\left(-\frac{\rho_{\mathsf{th}}}{\rho_0(\sigma_{\mathsf{D},\mathsf{R}_1}+\sigma_{\mathsf{D},\mathsf{R}_2})}\right)}{\sigma_{\mathsf{D},\mathsf{R}_1}\sigma_{\mathsf{D},\mathsf{R}_2}}\right]$$

$$\times\frac{\frac{\rho_{\mathsf{th}}}{\rho_0}\left(\sigma_{\mathsf{D},\mathsf{R}_1}+\sigma_{\mathsf{D},\mathsf{R}_2}+\frac{\rho_{\mathsf{th}}}{\rho_0}\right)\mathrm{Ei}\left(\frac{\rho_{\mathsf{th}}}{\rho_0\sigma_{\mathsf{D},\mathsf{R}_1}}\right)-\sigma_{\mathsf{D},\mathsf{R}_1}\left(\sigma_{\mathsf{D},\mathsf{R}_2}+\frac{\rho_{\mathsf{th}}}{\rho_0}\right)\exp\left(-\frac{\rho_{\mathsf{th}}}{\rho_0\sigma_{\mathsf{D},\mathsf{R}_1}}\right)+\sigma_{\mathsf{D},\mathsf{R}_1}\sigma_{\mathsf{D},\mathsf{R}_2}}{\sigma_{\mathsf{D},\mathsf{R}_1}\sigma_{\mathsf{D},\mathsf{R}_2}}$$

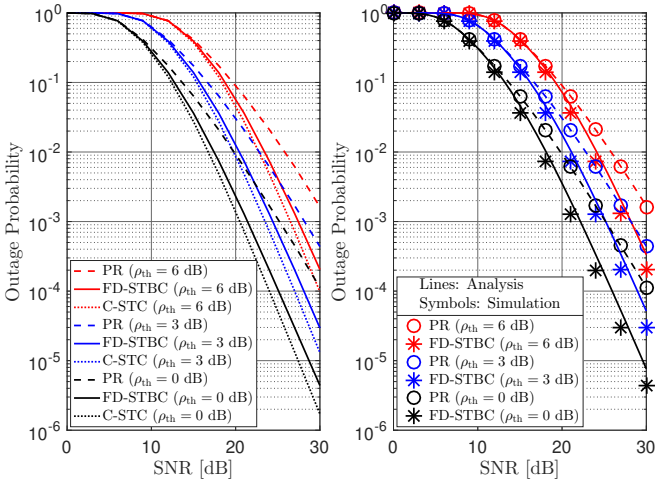

(a) Monte-Carlo simulation (b) Mathematical analysis

Fig. 3. End-to-end outage probability of the PR-based BRN, the FD-STBC-based BRN, and the C-STC-based BRN in a diamond-shaped four-node CBR.

proposed FD-STBC-based BRN is obtained. Moreover, substituting (14) instead of (15), the end-to-end outage probability closed-form for the conventional BRN is achieved.

IV. Simulation Results

We present the end-to-end outage probability performance of the proposed FD-STBC-based BRN and verify the analytical expression in Section III through Monte-Carlo simulations. As described in Section II, we consider a four-node CBR in a two-dimensional plane. In particular, two network topologies are considered: a line-shaped CBR, where the nodes are equally spaced on a line as $\mathsf{S}:[0,0]$, $\mathsf{R}_1:[1,0]$, $\mathsf{R}_2:[2,0]$, and $\mathsf{D}:[3,0]$, and a diamond-shaped CBR, where the nodes are located at $\mathsf{S}:[0,0]$, $\mathsf{R}_1:[1.5,0.5]$, $\mathsf{R}_2:[1.5,-0.5]$, and $\mathsf{D}:[3,0]$; where $\Psi:[\cdot,\cdot]$ represents the two-dimensional Cartesian coordinates of node $\Psi\in\{\mathsf{S},\mathsf{R}_1,\mathsf{R}_2,\mathsf{D}\}$. Also, the path loss exponent was set to $\alpha=3.5$ [11]. We benchmark the conventional PR-based BRN and the centralized STC (C-STC)-based BRN as comparative techniques. Here, the latter is that if both relays have successfully decoded the source packet at the end of the first slot, the two relays coordinate and transmit independent columns of $\mathcal{B}(\mathbf{x})$ to each other in the second slot. In other words, each relay mimics a specific array element (column) of the Alamouti code in (4).

Figs. 2 and 3 show the end-to-end outage probabilities of the proposed FD-STBC-based BRN, the conventional PR-based BRN, and the C-STC-based BRN with respect to the transmit SNR ρ_0 for three values of the threshold $\rho_{\mathsf{th}}\in\{0,3,6\}$ dB in the line-shaped CBR and the diamond-shaped one, respectively. In each figure, Figs. (a) and (b) represent the results of Monte-Carlo simulations and mathematical analyses, respectively. It is noteworthy that FD-STBC-based BRNs remarkably outperform existing PR-based BRNs regardless of topology, even though there are only two relays in the network. These results state that in practical military tactical MANETs, the proposed FD-STBC-based BRN can operate with higher energy efficiency under the same target reliability requirements and achieve better outage probability performance given the same transmission power than conventional BRNs. The C-STC-based BRN shows the best performance in all cases, but inter-node communication is required to acquire the activity of each node and coordinate the array elements. This will result in significantly higher signaling overhead and latency in large-scale or massive BRNs. Somewhat interestingly, we can observe that the proposed FD-STBC-based BRN achieves comparable performance to the C-STC-based BRN, even though it is a fully decentralized scheme. Finally, we can

observe from Figs. 2b and 3b that the analytical results match well with the simulations. This result reveals that the mathematical expression can represent the upper bound of the end-to-end outage probability of the FD-STBC-based BRN.

V. Conclusion

We have applied a fully distributed space-time block coding (FD-STBC) scheme to the barrage relay network (BRN) and validated its effectiveness by comparing the outage probability performance with the existing BRN. Briefly, the source broadcasts an information-bearing message in the first slot of a TDMA frame. The relays that have reliably decoded the source message then rebroadcast it with FD-STBC. In particular, we have employed a randomization matrix for the FD-STBC in which each column is independently and randomly selected on the surface of a complex unit hypersphere. Simulation results have shown that the proposed FD-STBC-based BRN significantly outperforms the conventional PR-based BRN and achieves comparable performance to the centralized STC-based BRN. We also have mathematically analyzed the upper bound of the end-to-end outage probability of the proposed FD-STBC-based BRN in the four-node CBR and verified it through computer simulations. We conclude that FD-STBC is considerably effective as an underlying technique for BRNs. In particular, the proposed FD-STBC-based BRN can be directly extended to any BRN. As a further study, we will generalize the proposed framework to arbitrary BRNs with more nodes and various topologies and analyze the system performance.

References

[1] J. L. Burbank, P. F. Chimento, B. K. Haberman, and W. T. Kasch, "Key challenges of military tactical networking and the elusive promise of MANET technology," *IEEE Commun. Mag.*, vol. 44, no. 11, pp. 39–45, Nov. 2006.

[2] K. Poularakis, G. Iosifidis, and L. Tassiulas, "SDN-enabled tactical ad hoc networks: Extending programmable control to the edge," *IEEE Commun. Mag.*, vol. 56, no. 7, pp. 132–138, Jul. 2018.

[3] S. Lee, J. Youn, and B. C. Jung, "A cooperative phase-steering technique in spectrum sharing-based military mobile ad hoc networks," *ICT Exp.*, vol. 6, no. 2, pp. 83–86, Jun. 2020.

[4] Y. Papageorgiou, M. Karaliopoulos, and I. Koutsopoulos, "Joint controller placement and TDMA link scheduling in SDN-enabled tactical MANETs," in *Proc. IEEE Military Commun. Conf. (MILCOM)*, Rockville, MD, USA, 2022, pp. 125–132.

[5] T. R. Halford and K. M. Chugg, "Barrage relay networks," in *Proc. 2010 Inf. Theory and Appl. Workshop*, La Jolla, CA, USA, 2010, pp. 1–8.

[6] A. Kott, A. Swami, and B. J. West, "The internet of battle things," *Computer*, vol. 49, no. 12, pp. 70–75, Dec. 2016.

[7] T. Abdelzaher, *et al.*, "Toward an internet of battlefield things: A resilience perspective," *Computer*, vol. 51, no. 11, pp. 24–36, Nov. 2018.

[8] C. Yu, S. Shen, H. Yang, K. Zhang, and H. Zhao, "Leveraging energy, latency, and robustness for routing path selection in internet of battlefield things," *IEEE Internet Things J.*, vol. 9, no. 14, pp. 12 601–12 613, Jul. 2022.

[9] A. Blair, T. Brown, K. M. Chugg, T. R. Halford, and M. Johnson, "Barrage relay networks for cooperative transport in tactical MANETs," in *Proc. IEEE Military Commun. Conf. (MILCOM)*, San Diego, CA, USA, 2008, pp. 1–7.

[10] T. R. Halford, K. M. Chugg, and A. Polydoros, "Barrage relay networks: System & protocol design," in *Proc. IEEE Int. Symp. Pers. Indoor Mobile Radio Commun. (PIMRC)*, Istanbul, Turkey, 2010, pp. 1133–1138.

[11] S. Talarico, M. C. Valenti, and T. R. Halford, "Unicast barrage relay networks: Outage analysis and optimization," in *Proc. IEEE Military Commun. Conf. (MILCOM)*, Baltimore, MD, USA, 2014, pp. 537–543.

[12] ——, "Controlled barrage regions: Stochastic modeling, analysis, and optimization," in *Proc. IEEE Military Commun. Conf. (MILCOM)*, Baltimore, MD, USA, 2016, pp. 466–472.

[13] N. Woolsey, M. Ji, and B. Kraczek, "Predicting needs in future decentralized networks through analysis of barrage relay networks," in *Proc. IEEE Wireless Commun. Netw. Conf. (WCNC)*, Nanjing, China, 2021, pp. 1–6.

[14] B. Kraczek and N. Woolsey, "Geometry-informed transmission strength scaling in barrage relay networks," in *Proc. IEEE Military Commun. Conf. (MILCOM)*, San Diego, CA, USA, 2021, pp. 690–695.

[15] W. Son, J. Choi, S. Park, H. Lee, and B. C. Jung, "A time synchronization protocol for barrage relay networks," *Sensors*, vol. 23, no. 5, p. 2447, Feb. 2023.

[16] B. Sirkeci-Mergen and A. Scaglione, "Randomized space-time coding for distributed cooperative communication," *IEEE Trans. Signal Process.*, vol. 55, no. 10, pp. 5003–5017, Oct. 2007.

[17] J. N. Laneman and G. W. Wornell, "Distributed space-time-coded protocols for exploiting cooperative diversity in wireless networks," *IEEE Trans. Inf. Theory*, vol. 49, no. 10, pp. 2415–2425, Oct. 2003.

[18] S. Yiu, R. Schober, and L. Lampe, "Distributed space-time block coding," *IEEE Trans. Commun.*, vol. 54, no. 7, pp. 1195–1206, Jul. 2006.

[19] T. Q. Duong, Ö. Alay, E. Erkip, and H. -J. Zepernick, "End-to-end performance of randomized distributed space-time codes," in *Proc. IEEE Int. Symp. Pers. Indoor Mobile Radio Commun. (PIMRC)*, Istanbul, Turkey, 2010, pp. 988–993.

[20] J. Soffritti, T. Q. Duong, M. L. Merani, and H. -J. Zepernick, "Performance analysis of randomized distributed space-time codes over composite gamma/lognormal fading channels," in *Proc. IEEE 80th Veh. Technol. Conf. (VTC2014-Fall)*, Vancouver, BC, Canada, 2014, pp. 1–5.

[21] Y. -B. Kim, K. Yamazaki, and B. C. Jung, "Virtual full-duplex cooperative NOMA: Relay selection and interference cancellation," *IEEE Trans. Wireless Commun.*, vol. 18, no. 12, pp. 5882–5893, Dec. 2019.

[22] J. Youn, J. S. Yeom, J. Joung, and B. C. Jung, "Cooperative space-time line code for relay-assisted internet of things," *ICT Exp.*, vol. 9, no. 2, pp. 253–257, Apr. 2023.

[23] D. K. Lee and K. M. Chugg, "A pragmatic approach to cooperative communication," in *Proc. IEEE Military Commun. Conf. (MILCOM)*, Washington, DC, USA, 2006, pp. 1–7.

[24] J. Joung, S. Park, J. -M. Oh, and E. -R. Jeong, "SNR threshold-based relay association and random phase rotation for cooperative communication," *IEEE Access*, vol. 11, pp. 24 794–24 807, 2023.